Determination of Hydrogen Peroxide in Milk by Fluorometric Method using Chitosan-Coumarin Film Sensor

K. Karimi^a, M. Gharachorloo^{a*}, A. Fallah^b

Received: 26 September 2025 Accepted: 10 October 2025

ABSTRACT: Accurate determination of hydrogen peroxide is of great importance from a public health standpoint. In this work, determination of hydrogen peroxide in milk was performed using chitosan-coumarin film sensor via a fluorometric method. Coumain-3-carboxylic acid (CCA) was used as a probe in the matrix of chitosan. The structures of the films were confirmed by various instrumental analysis including FT-IR, TGA, and SEM. Various parameters such as the amount of CCA, pH, and the effect of catalyst on the response of the sensor were investigated. The results indicated that ultraviolet radiation could improve the response of the sensor. Hydrogen peroxide was determined using this method in the range of 12-200 μ M and 0.5-8.0 mM. The calibration plots demonstrated that the fluorescence response of the sensor films was linear over hydrogen peroxide concentrations of 12-200 μ M and 500-8000 μ M, with a detection limit (LOD) of 3 μ M.

Keywords: Chitosan, Hydrogen Peroxide, Milk, Photoluminescence, Sensor.

Introduction

Food safety is a critical public issue. The primary goal is to control hazards, including biological, chemical, and physical contaminants. Effective controls are essential at all stages of the food chain, from production consumption (Gizaw, 2019). Hydrogen peroxide (H_2O_2) significant has importance in food safety due to its powerful antimicrobial properties. It acts as a disinfectant and sterilizing agent, to eliminate bacteria, viruses, and molds. Consequently, it is applied in various food

^a PhD Student of the Department of Food Science and Technology, SR.C., Islamic Azad University, Tehran, Iran.

 ^a Professor of the Department of Food Science and Technology, SR.C., Islamic Azad University, Tehran, Iran.
 ^b Associate Professor of Department of Statistics, Imam Khomeini International University, Qazvin, Iran.

industry processes, such as the aseptic packaging of dairy products and the sanitization of food contact surfaces. Therefore, monitoring hydrogen peroxide is crucial in certain foods (Sadowska-Bartosz & Bartosz, 2025). Excessive levels of hydrogen peroxide may indicate spoilage or pose a safety risk to consumers. Hydrogen peroxide can enter the milk at any stage of milking, transportation and processing (Ivanova et al., 2019). In some countries, H₂O₂ may be added to raw milk as a preservative (10-15 mM) (Walstra et al., 2006), but it can be removed before milk processing by adding catalase. In addition, hydrogen peroxide

^{*}Corresponding Author: maryam.gharachorloo@iau.ac.ir

may be added as an adulterating agent to increase the shelf life of milk. The presence of hydrogen peroxide in food products can lead to serious health problems for humans. Various methods have been applied for determination of hydrogen peroxide in milk, including amperometric detection (Guascito et al., 2008), Polarography (Domergue et. al., 2023), colorimetric detection (Nitinaivinii et. al., 2014), high performance liquid chromatography (HPLC) (Ivanova et al., 2019), fluorescence method (Abo et al., 2011), chemiluminescence (Vasconcelos et al., 2023), spectroscopic methods, chemometrics methods, and use chemical sensors (Shariati-Rad et al., 2017). Photoluminescence methods offer significant advantages for chemical sensing. They provide high sensitivity, excellent selectivity, rapid measurements, and allow for non-destructive analysis. Furthermore, the technique can be adapted for real-time monitoring (Wang et al., 2013). These benefits make photoluminescence a powerful tool for various applications. Chemical sensors are of critical importance for monitoring and analysis of numerous fields (Kim et al., 2024). The important factors that should be considered for design of a chemical sensor are sensitivity, limit of detection (LOD), selectivity, response time, stability reproducibility, real-world applicability, simplicity and cost. For food safety, they monitor quality and spoilage. A key advantage of chemical sensors is their potential for real-time, on-site analysis. This eliminates the need for timeconsuming laboratory tests. While several methods exist for hydrogen peroxide detection, many are complex, consuming, or unsuitable for application in food matrices like milk. Therefore, the development of sensitive and selective chemical sensors is essential

for advancing public health, safety, and technological innovation.

In this study, we aimed to develop a novel, fluorescence-based sensor for the detection of hydrogen peroxide in milk. This was achieved by synthesizing a chemical film sensor based on chitosan and coumarin carboxylic acid. Chitosan is a natural biopolymer derived from chitin. It is its biocompatibility, known for biodegradability, and low toxicity (Thambiliyagodage et al., 2023). It serves as an excellent matrix for developing chemical sensors and active packaging materials. Its versatility makes valuable polymer for enhancing food safety and quality. The proposed sensor is unique due to its high selectivity, simplicity, and applicability to complex food samples like milk. The paper details the sensor fabrication, optimization of analytical parameters, and its successful application in spiked milk samples. The key advantage of this approach is its ability to perform measurements directly in milk with minimal sample preparation, addressing a significant need for on-site food safety monitoring. The analytical performance (LOD, LOQ, linear range), and recovery studies in milk samples were also discussed.

Materials and Methods

- Materials

Chitosan (High molecular weight, MW=310-375 kDa, and 75-85% DD), gelatin, CCA, copper (II) sulfate, cobalt (II) sulfate, manganese (II) sulfate, and zinc sulfate were prepared from Sigma-Aldrich Co. Nicke l(II) sulfate, iron (II) sulfate, cadmium sulfate, and silver nitrate was obtained from Merck Millipore.

- Instrumental characterization

The FT-IR of the samples (in the form of KBr tablets) were obtained by an Bruker

infrared spectrometer, Tensor 27, Germany. The fluorescence spectra were acquired using a Hitachi fluorescence spectrometer, F-2700, Japan. The UV-Vis spectra were achieved using a CamSpec optical spectrometer, M350, England. In order to homogenize the solutions an ultrasonic bath (340 Watts, WiseClean, 50 Hz) was used. Surface morphology of the samples was obtained by a ESEM (Quanta 200) after freeze-drying at -40°C by a freeze dryer (SBPE, Iran). TGA analysis was performed by a Perkin Elmer analyzer (Diamond Pyris, USA), under nitrogen atmosphere at a heating rate of 20 °C/min.

- Preparation of iron (II) sulfate solution

In order to prepare the iron (II) sulfate solution, 0.3 grams of iron (II) sulfate (FeSO₄) was accurately weighed using a balance and dissolved in a sufficient amount of distilled water in a beaker. The resulting solution was then transferred to a volumetric flask and brought to a volume of 500 mL by adding distilled water (Li *et al.*, 2025). Subsequently, determined volumes of this solution were used in each plate using a graduated pipette.

- Preparation of coumarin-3-carboxylic acid solution

In order to prepare the coumarin carboxylic acid solution, 0.10 g of coumarin-3-carboxylic acid was accurately weighed using a balance and dispersed in 40 mL of distilled water. While this mixture was being stirred using a magnetic stirrer, 1 mL of 1.0 M sodium hydroxide (NaOH) solution was added dropwise, and stirring of the resulting mixture continued until the sample was completely dissolved. It is necessary to heat the mixture gently (Islas *et al.*, 2018). The color of the solution becomes pale lemon-yellow. Then, determined volumes of this solution (including 1.0, 2.0, 3.0, and 4.0 mL) were

used in each plate.

- Preparation of the film sensor

Sensor films based on chitosancoumarin carboxylic acid were prepared by casting method (Myers et al., 2014). In a 100 mL beaker, specified amounts of a high molecular weight chitosan solution (30 mL, containing 0.375 g of chitosan) and a gelatin solution (7.0 mL, containing 0.075 g of gelatin) were combined in an 80:20 weight ratio (chitosan to gelatin). Next, a coumarin carboxylic acid solution (volumes of 1.0, 2.0, 3.0, or 4.0 mL) was added dropwise to the stirring mixture until it became completely homogeneous. While the solution was being vigorously stirred using a magnetic stirrer, 0.3 mL of an iron (II) sulfate solution was added dropwise to achieve a uniform mixture. The resulting solution was poured into a plastic plate and placed in an oven at 70°C for 3 days. After drying, the resulting films were transparent.

- Preparation of milk serum

In order to prepare the milk serum, 10.0 mL of the milk sample was first poured into each centrifuge tube and 120 microliters of acetic acid was added to each tube (Walstra *et al.*, 2006). The samples were then centrifuged at 6000 rpm for 15 minutes. The clear serum contents were then filtered using a 0.45 µm Teflon syringe filter. This step was performed to remove any suspended particles in the serum that might not have been separated during the centrifugation stage or that may have entered the serum during decanting Mukhopadhya *et al.*, 2021).

- Fluorescence Response Measurement

In order to measure the fluorescence response of the sensor films in a hydrogen peroxide solution, a specific amount (0.04 g) of each film was dispersed and dissolved in 10 mL of a determined concentration of hydrogen peroxide solution using a magnetic stirrer for one hour. Subsequently, the samples were placed inside a protective box under ultraviolet (UV) irradiation (100-watt mercury lamp) at a fixed distance. The fluorescence of solutions was measured at specific time intervals using an excitation wavelength of 350 nm.

Limit of detection and limit of quantification

The Limit of Detection (LOD) and the Limit of Quantification (LOQ) are defined as the minimum concentration of an analyte that can be reliably detected and quantified, respectively (Harris, 2007). For this purpose, the standard deviation of 10 blank samples was measured and averaged. The LOD was then calculated using equation 1.

$$LOD = 3S_b / m \tag{1}$$

In this equation, S_b is the standard deviation of the blank, and m is the slope of the calibration curve. The LOQ was calculated according to the following equation:

$$LOQ = 10S_b / m \tag{2}$$

The recovery experiment was applied to investigate the matrix effects (Harris, 2007), and calculated using the following equation:

$$R(\%) = (F - I) / A \times 100$$
 (3)

Where, A is the concentration of the analyte added to the solution, F is analyte concentration for spiked solution, and I is analyte concentration for unspiked solution (without the added analyte).

- Statistical Analysis

Each experiment was performed in

three to five replicates. The results are presented as the mean, standard deviation (SD), and relative standard deviation (RSD). In order to determine the limit of detection (LOD), each test was repeated 10 times, after which the standard deviation and mean were calculated. A one-way analysis of variance (ANOVA) was used to compare the means. Data analysis was performed using SPSS software (version 20) with a significant level of p < 0.05.

Results and Discussion

- Synthesis and characterizations

prepare chitosan-coumarin carboxylic acid-based sensor films (Cs/Ge-Fe-CCA), high molecular weight chitosan and gelatin were used. Gelatin was employed to reduce the viscosity of the chitosan solution, facilitate the sample preparation process, and improve the properties of the films. Iron ions act as a catalyst and facilitate the formation of hydroxyl radicals in reaction peroxide. hydrogen The H_2O_2 concentration was determined using a fluorometric method based on hydroxyl radical-mediated oxidation of coumarin-3-carboxylic acid (CCA). CCA was selected as a suitable fluorophore agent. This compound reacts with the hydroxyl radical to form 7-hydroxy-CCA, which produces fluorescence emission in the range of 400-500 nm with an excitation wavelength of around 350 nm The (Figure 1). structure of synthesized sensor film was studied by FT-IR spectroscopy. Chitosan characteristic absorptions appeared in the region of 3600-13200 cm-1, 1657 cm-1, 1600 cm-1, 1417 cm-1, and 1092 cm-1, which are related to the stretching vibrations of the H-O and H-N bonds. stretching vibrations of the carbonyl group correspond to the remaining acetyl group,

the bending vibrations of the H-N bond, the bending vibrations of the H-C bond, and the stretching vibrations of the C-O respectively bond, (Figure comparison of the FT-IR spectra related to chitosan and the sensor film prepared based on chitosan- coumarin carboxylic acid shows that the bandwidth in the region of 800-2000 cm⁻¹ has changed. This indicates an alteration in the intermolecular hydrogen bonds of chitosan due to its interaction with gelatin and carboxylic acid groups of CCA.

The surface morphology of the sensor film was studied using a scanning electron microscope (SEM). Before imaging, the samples were first swollen in an aqueous environment and then dried using a freeze dryer at -70°C. As shown in Figure 3, the films have a porous structure, which is likely due to swelling in the aqueous environment. The X-ray mapping image of the sensor film shows a uniform distribution of ions throughout the film structure.

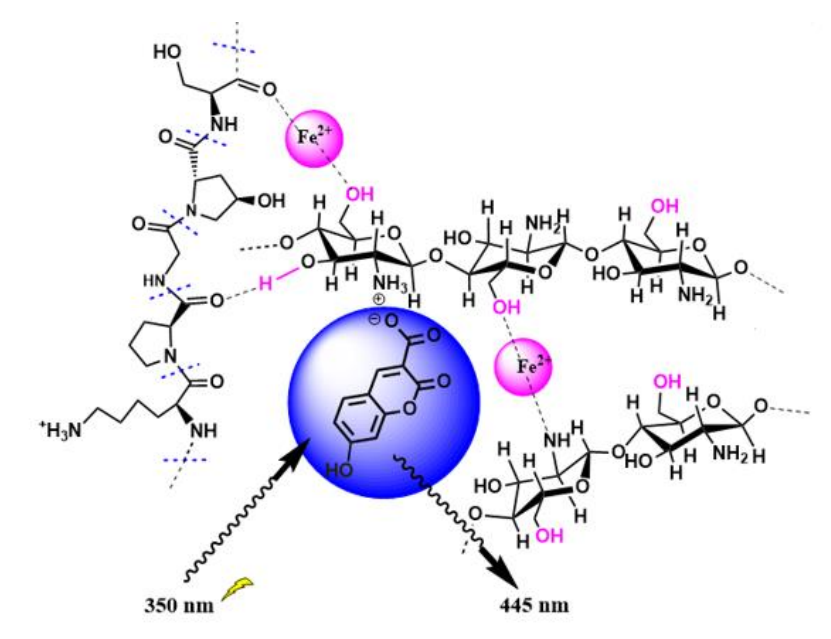


Fig. 1. The proposed structure of the film sensor and fluorescence emission at 445 nm.

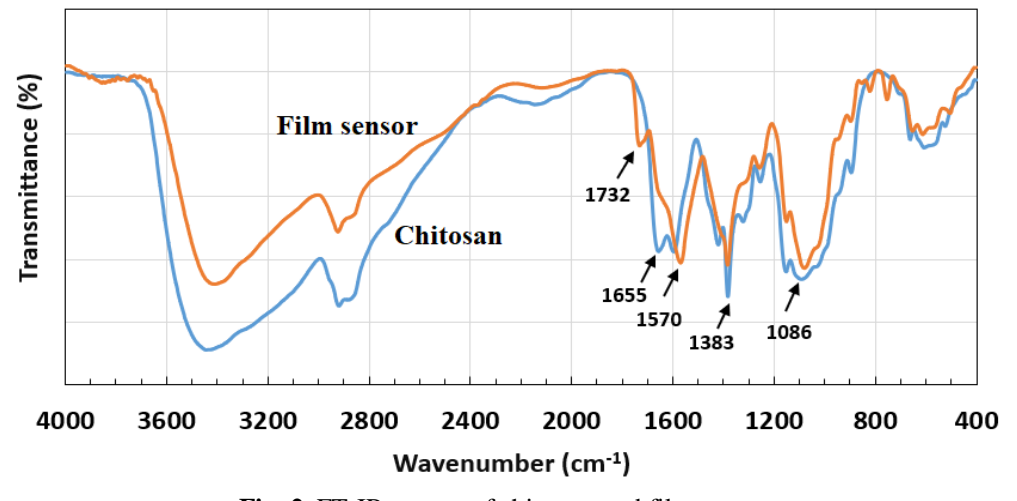


Fig. 2. FT-IR spectra of chitosan, and film sensor.

Thermogravimetric analysis (TGA) of the sensor film compared to chitosan is shown in Figure 4. The initial weight loss of the samples up to approximately 120 °C is related to the evaporation of water. Chitosan shows a 30–35% weight loss between 200–350 °C, which corresponds to the thermal degradation of the polymer

backbone (through depolymerization and deacetylation). An additional weight loss of 20–30% above 400 °C up to 800 °C is due to carbonization and the breakdown of residual organic matter. Introducing Fe²⁺ ions into the chitosan films shifts the onset temperature of thermal degradation to a lower range.

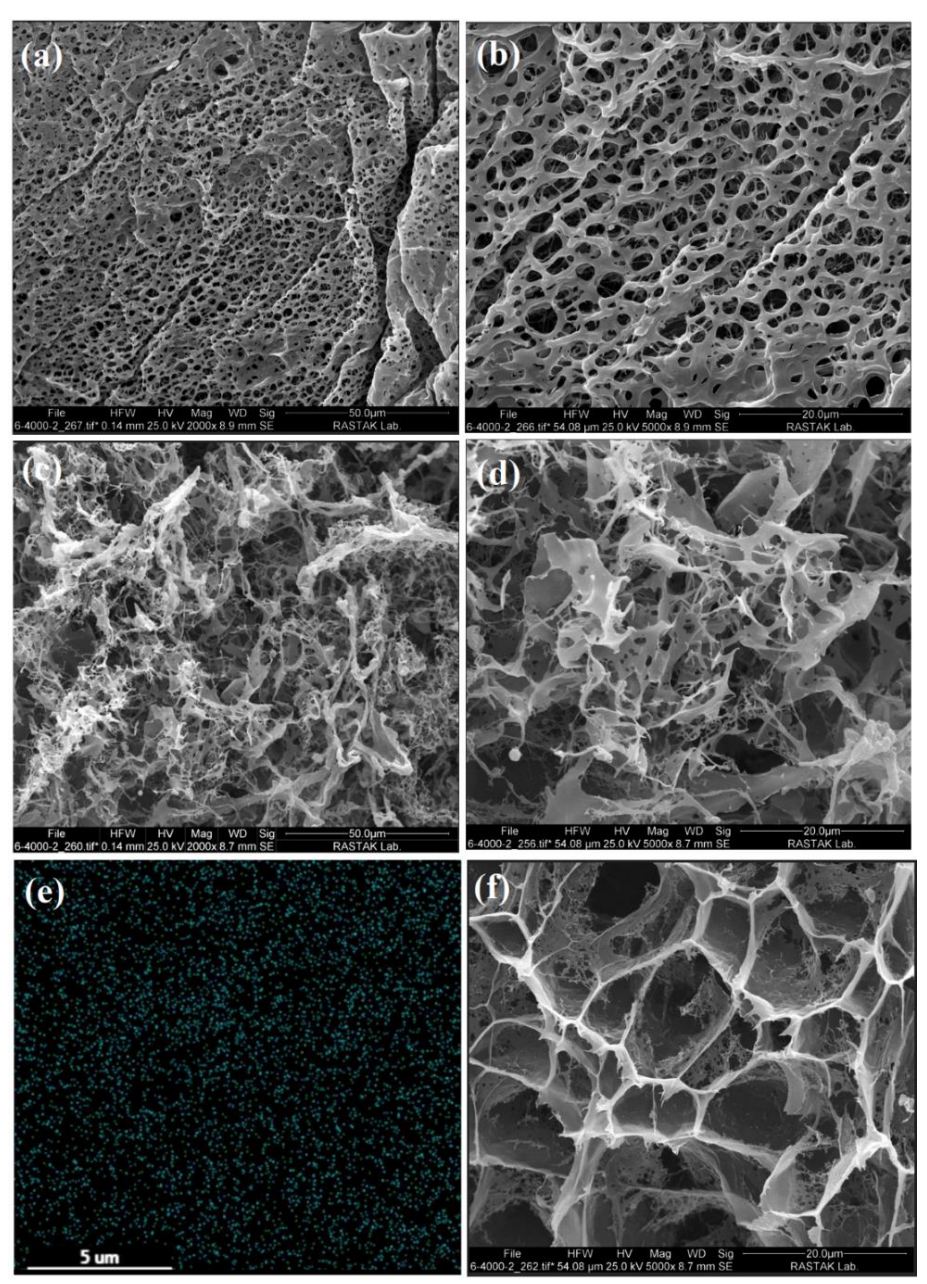


Fig. 3. SEM images of Cs/Ge-CCA films with magnification of 2000x and 5000x (a,b), Cs/Ge-Fe-CCA film sensor with magnification of 2000x and 5000x (c,d), X-ray mapping analysis for the dispersion of iron ions (e), the sensor contains iron catalyst (with a concentration of 10^{-4} molar) with magnification of 5000x (f), after freeze-drying.

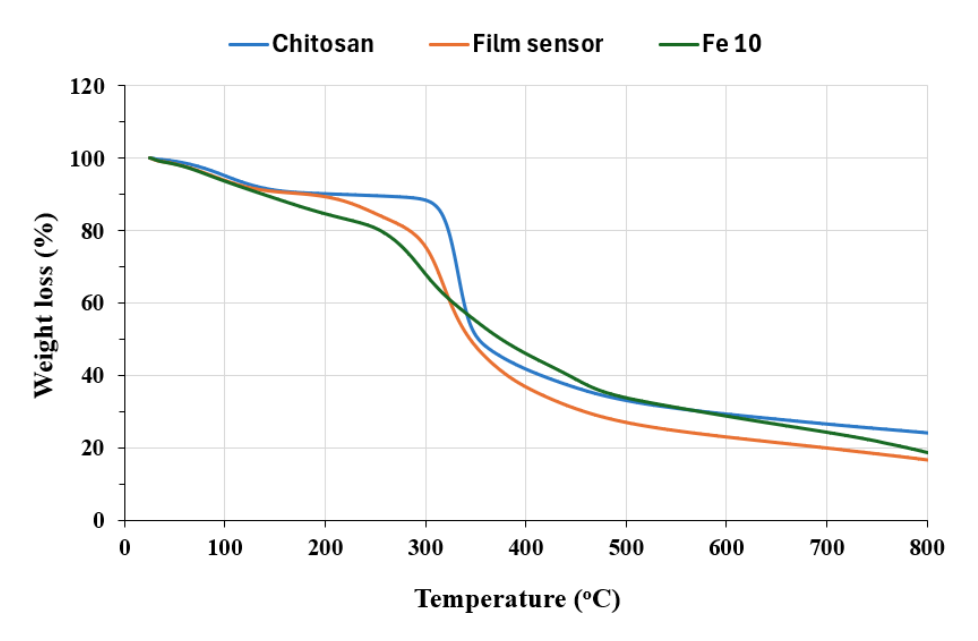


Fig. 4. TGA of the sensor film compared to the chitosan, and sensor film contains iron catalyst (with a concentration of 10⁻⁴ molar, Fe10).

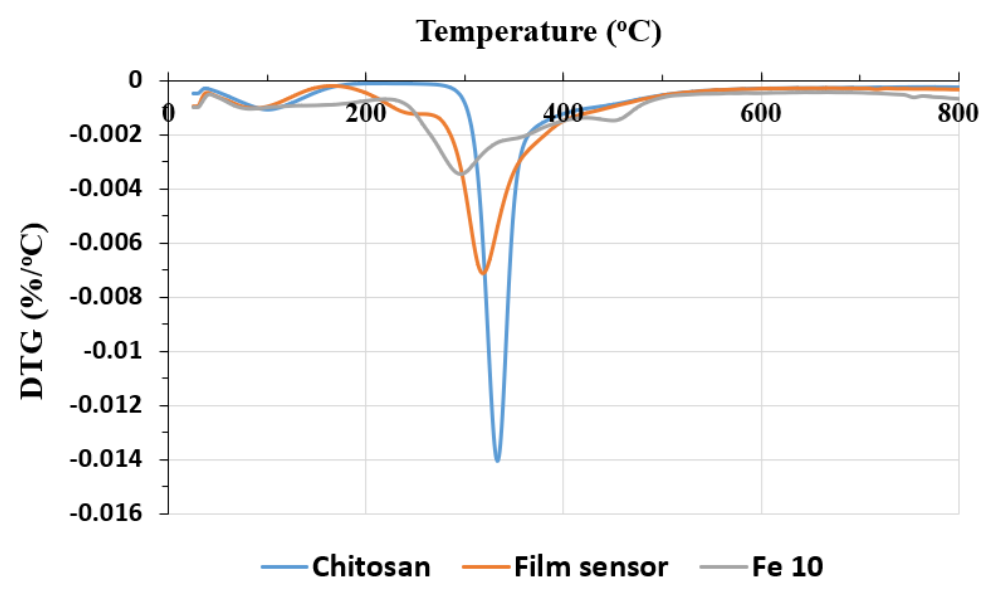


Fig. 5. DTG of the sensor film compared to the chitosan, and sensor film contains iron catalyst (with a concentration of 10^{-4} molar, Fe10).

This phenomenon is attributed to the interaction between Fe2⁺ ions and the functional groups of chitosan, particularly the amino and hydroxyl groups. The ions can form complexes with chitosan, reducing the energy required to break its chemical bonds. Furthermore, Fe2⁺ ions may act as catalysts, accelerating the

decomposition process and thereby lowering the degradation onset temperature. Consequently, the presence of transition metals like iron tends to reduce the overall thermal stability of the film compared to pure chitosan.

However, while Fe²⁺ ions initially lower the onset temperature, increasing

their concentration can enhance thermal stability at higher temperatures (e.g., above 400 °C). At these high temperatures, the ions may form iron oxides within the matrix, which act as thermal insulators and stabilize the charred structure (Figure 4, Fe10). In the DTG analysis, pure chitosan typically exhibits a sharp degradation peak due to its relatively loose polymer structure (Figure 5). In contrast, the chitosan-iron film exhibits a broader and shifted peak, indicating a slower and more gradual degradation process. This slower degradation rate is due to Fe²⁺ coordination interactions: ions coordinate with the amino and hydroxyl groups in chitosan, creating a cross-linked structure. This structure reduces polymer chain mobility, increasing the thermal resistance of the polymer chains to breakdown.

Effect of the amount of coumarin carboxylic acid

The effect of the amount of coumarin carboxylic acid on the fluorescence response of the films was investigated (Figure 6). The results showed that the fluorescence response of the films increases by increasing the amount of carboxylic coumarin acid approximately 1.25% by weight. This is attributed to the increased population of fluorescent molecules. The decrease in the fluorescence response of the films with further increase in coumarin carboxylic acid beyond 1.25% by weight is related to reaction of 7-hydroxycoumarin carboxylic acid with the hydroxyl radical (Rutely, et al., 2018). Therfore, the amount by weight of coumarin of 1.25% carboxylic acid was selected as the optimal value.

- Effect of catalyst

The effect of the type of metal ions as catalysts on the response of the sensors was investigated. The results are presented in Figure 7. The highest response was obtained in the presence of iron ions. The classic Fenton reaction describes the activation of hydrogen peroxide (H₂O₂) by ferrous ions (Fe²⁺) to generate hydroxyl radicals through a complex reaction sequence (Fig. 8).

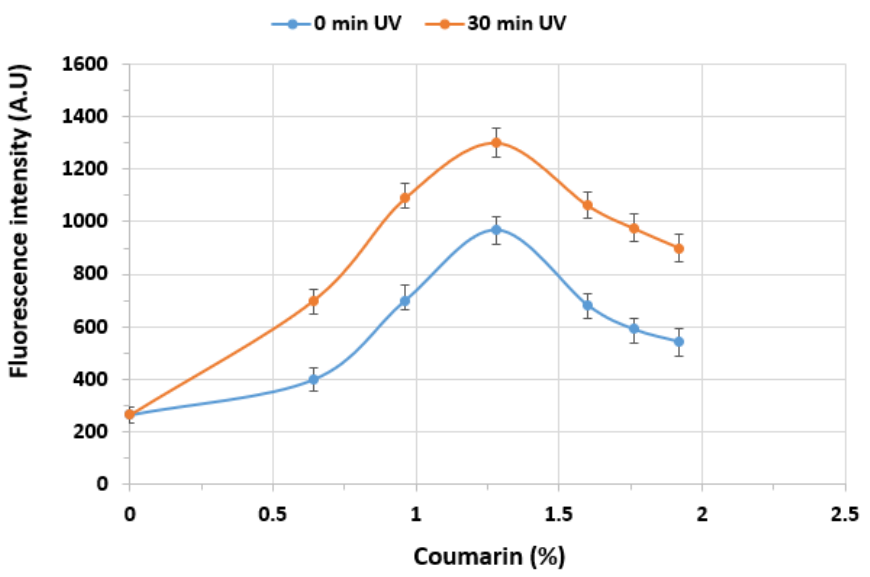


Fig. 6. The effect of the amount of coumarin carboxylic acid on the fluorescence response of the films in the presence or absence of UV (H₂O₂ 1.0 mM, irradiation time 30 min, and Ex. 360 nm).

- Effect of pH

The pH of a solution is one of the important factors in the study fluorescence systems. Therefore, the fluorescence intensity of the prepared films was investigated as a function of pH. The results are presented in Figure 9. As shown in this figure, the highest response is observed at pH = 3. Coumarin-3carboxylic acid exhibits a protonationdeprotonation equilibrium with pKa = 3.3– 3.7 due to the presence of the carboxyl group (Nafradi et al., 2020). Therefore, at pH = 3, the protonated form of coumarin-3-carboxylic acid is dominant, which shows the highest fluorescence intensity. it is observed that with a further decrease in pH, the fluorescence intensity decreases again with a milder slope. The results of the ANOVA statistical test indicate that there is a significant difference between the various catalyst groups.

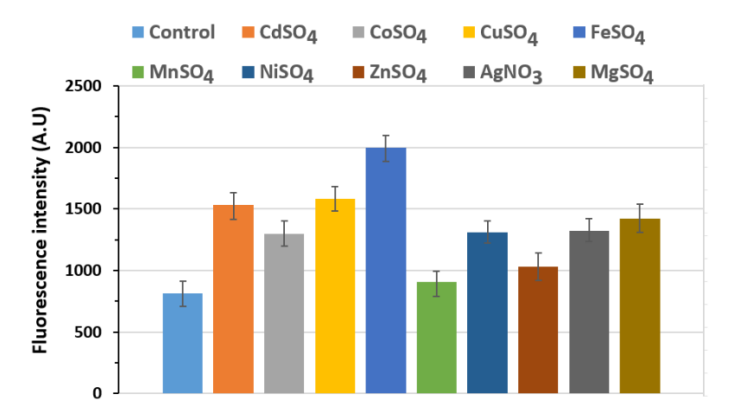


Fig. 7. Effect of catalyst on the fluorescence response of the film sensor (H₂O₂ 2.0 mM, irradiation time 35 min, Ex. 360 nm.)

$$Fe^{2^{+}} + H_{2}O_{2} \rightarrow Fe^{3^{+}} + HO^{\bullet} + OH^{-}$$
 $(k = 63-76 \text{ M}^{-1}\text{s}^{-1})$
 $Fe^{3^{+}} + H_{2}O_{2} \rightarrow Fe^{2^{+}} + HO_{2}^{\bullet} + H^{+}$ $(k = 0.001-0.01 \text{ M}^{-1}\text{s}^{-1})$

Fig. 8. The reaction of iron ions with hydrogen peroxide and the formation of hydroxyl radicals.

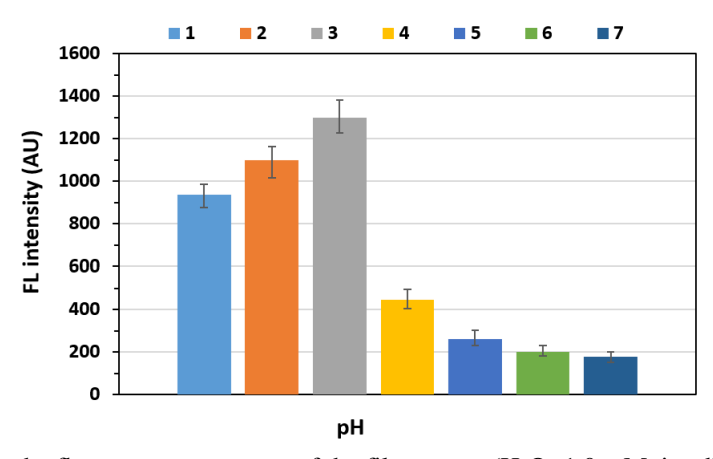


Fig. 9. Effect of pH on the fluorescence response of the film sensor (H_2O_2 1.0 mM, irradiation time 30 min, Ex. 360 nm.

-Effect of irradiation time

Coumarins are known as light-sensitive aromatic compounds and can undergo photoexcitation in the presence ultraviolet light (Zhou et al., 2024). The fluorescence response of the sensors to different concentrations of hydrogen peroxide was investigated. Figure 10 shows that the fluorescence response significantly increases with extended ultraviolet irradiation time, reaching its maximum after approximately 45 minutes. Then, it slightly decreases with further irradiation. The production of hydroxyl radicals increases with increasing the ultraviolet irradiation intensity, leading to a higher concentration of 7-hydroxy coumarin carboxylic acid. The decrease in fluorescence intensity after 45 minutes can be attributed to the reaction of 7hydroxycoumarin carboxylic acid with hydroxyl radicals, which competes with the formation of 7-hydroxycoumarin and leads to a reduction in the population of fluorescing molecules (Rutely et al., 2018). Calibration plots established a linear relationship between the fluorescence response of the produced sensor films and hydrogen peroxide

concentrations in the ranges of 12-200 μM and 500-8000 μM . The statistical analysis results demonstrate a very strong correlation between the hydrogen peroxide concentration and the fluorescence response of the sensor (R=0.96, R=0.99). The obtained model is also statistically highly significant (p<<0.05).

- Selectivity in milk samples

The selectivity of the sensor towards hydrogen peroxide and other additives was investigated. To evaluate selectivity, the response of the sensor in milk serum was tested against various types of substances that are the most common additives in milk adulteration. The results showed that the sensor is highly selective for hydrogen peroxide, and its response to other compounds is very weak (Figure 11). Statistical analysis (ANOVA) indicates that the response of the sensor to hydrogen peroxide is significantly different from its response to other substances 0.05). (p << demonstrating that the sensor has very high selectivity for hydrogen peroxide and can effectively distinguish it from other additives in milk.

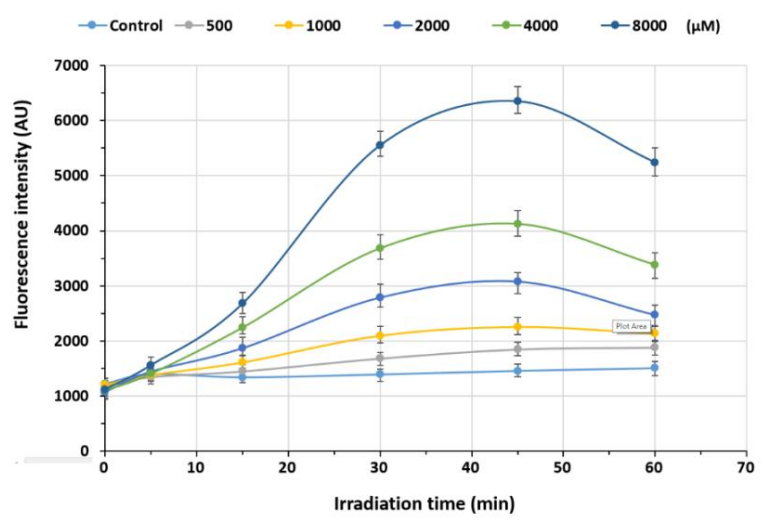


Fig. 10. The fluorescence response of film sensor to different concentrations of hydrogen peroxide under UV irradiation at pH=3.

- Recovery test in milk samples

Recovery tests are typically performed to investigate the effect of the real sample matrix on the response of sensor (Ardila et al., 2013). The recovery experiment was conducted to evaluate the effect of the milk serum matrix on the response of the sensor (Table 1). Hydrogen peroxide was selected at three different concentrations and added to the milk samples. The recovery of hydrogen peroxide obtained in the range of 97% to 105% for the samples. The relative standard deviation (RSD) is less than 5%, indicating that the fluorescence sensor has good reliability for measuring hydrogen peroxide in milk samples.

- Comparison with other sensors

Table 2 shows the performance of the produced sensor, compared to a number of other hydrogen peroxide sensors. Typically, comparable parameters include the detection range or linear range, detection limit, sensor response speed, and selectivity. An ideal sensor possesses a wide detection range, a low detection limit, a fast response speed, and high selectivity. As shown, the developed sensor demonstrates competitive performance for hydrogen peroxide detection. Furthermore, it functions well over a wide range of concentrations, which is of great practical importance.

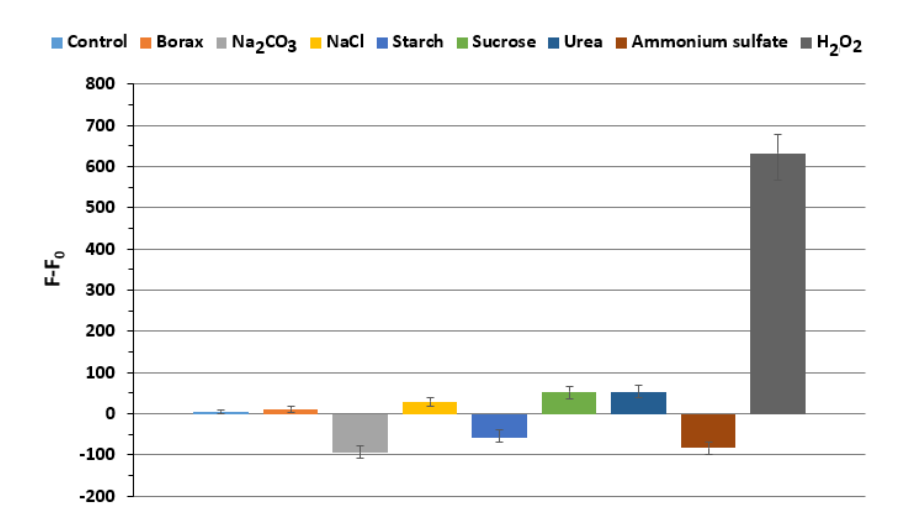


Fig. 11. Selectivity of the sensor towards hydrogen peroxide (H₂O₂ 2.0 mM, irradiation time 30 min, Ex. 360 nm, additive 5 mM).

Table 1. The results of the recovery tests in milk samples

Milk sample	Added (µM)	Found (µM)	R.S.D (%)	Recovery (%)
M1	1000	1051	4.6	104.8
	2000	1953	3.1	97.5
	4000	4074	2.17	101.7
M2	1000	1035	4.96	103.2
	2000	2096	3.5	104.75
	4000	3937	2.8	98.3
M3	1000	990	4.72	98.8
	2000	2081	2.83	103.9
	4000	4078	2.65	101.8

Tabl 2. Comparison of the Cs/Ge-Fe-CCA film sensor with the other sensors

Sensor/Biosensor	Type	LOD (µM)	Detection Range (mM)	RT	Selectivity	Ref.			
HRP/Luminol sensor	Ch	4.6	0.01-0.5	fast	-	Zambrano <i>et al.</i> , 2020			
Composite of pyrite and silver nanoparticle	Е	20	0.1-30	fast	✓	Zhao <i>et al.</i> , 2021			
MgO based nonenzymatic sensor	E	3.3	0.05-0.2 0.2-10	fast	✓	Dong <i>et al.</i> , 2015			
rGO-MoS ₂ on PTE screen-printed electrode	Е	0.046	0.001-0.05	fast	✓	Palsaniya <i>et</i> al., 2023			
I ⁻ /TMB platform	C	1.1	0.0017-0.167	within 3 min	-	Wang <i>et al</i> ., 2019			
Bioactive paper strip sensor (Guaiacol +HRP)	C	0.35	1.25-15	slow	low	Lima <i>et al</i> ., 2020			
Nano-composites of MoS ₂ nanosheets and CNT in the presence of TMB	C	1.4	0.005-0.5	slow	✓	Zhang <i>et al.</i> , 2022			
Cupric oxide nanoparticles and terephthalic acid	F	0.34	0.005-0.2	fast	✓	Hu <i>et al</i> ., 2014			
Nanohybrid of carbon dots and nanoceria (CeO ₂)	F	0.047	0.0001-0.1	fast	✓	Liu <i>et al.</i> , 2022			
Cs/Ge-Fe-CCA film sensor	F	3	0.012-0.2 0.5-8	fast	✓	This work			

Conclusion

In this work a novel film sensor (CS/Ge-Fe-CCA) was designed determination of hydrogen peroxide in milk by a fluorometric method using a photo-Fenton-like process. The use of the sensors provides a rapid method for measuring hydrogen peroxide with high photo-Fenton sensitivity using a mechanism. Uniform distribution of iron ions in the film structure was demonstrated by X-ray mapping. The results showed that by increasing the iron ion catalysts up to an optimal value (10^{-5} M) , the fluorescence response of the sensors increases. Furthermore, ultraviolet irradiation has a significant impact on the response of the sensors. The optimal UV irradiation time for the sensors was 45 minutes. The prepared sensor films were compared with other sensors for hydrogen peroxide detection. The results showed that the produced sensors have very high hydrogen selectivity for detecting peroxide. The practical value of the fluorescent sensors was demonstrated by their application in detecting hydrogen peroxide in milk samples. However, the fluorescent sensor has limitations in real samples at very low hydrogen peroxide concentrations due to the matrix effect. Consequently, in milk samples, sensitivity of the sensor depends on the degree of milk filtration. The recovery of hydrogen peroxide was obtained in the range of 97% to 105% for the samples. The relative standard deviation (RSD) is less than 5%, indicating that the produced fluorescent have good reliability measuring hydrogen peroxide. Among the advantages of the sensor are simple preparation, low cost, high sensitivity, biocompatibility, fast response, good stability, and the synergistic effect of ultraviolet irradiation. Other characteristics of these sensors, such as their shelf life, high sensitivity, and rapid response, suggest that the sensor is suitable for the rapid and accurate detection of hydrogen industries, peroxide in different particularly in the food industry.

References

Abo, M., Urano, Y., Hanaoka, K., Terai, T., Komatsu, T. & Nagano, T. (2011). Development of a highly sensitive fluorescence probe for hydrogen peroxide, *Journal of the American Chemical Society*, 133(27), 10629–10637. https://doi.org/10.1021/ja203521e

Ardila, J. A., Oliveira, G. G., Medeiros, R. A. & Fatibello-Filho, O. (2013). gemfibrozil Determination of pharmaceutical and urine samples by square-wave adsorptive stripping using voltammetry carbon a glassy modified multi-walled electrode with carbon nanotubes within a dihexadecyl hydrogen phosphate film, Journal of Electroanalytical Chemistry, 690, 32-37. https://doi.org/10.1016/j.jelechem.2012.11. 038

Domergue, L., Cimetière, N., Giraudet, S. & Hauchard, D. (2023). Determination of hydrogen peroxide by differential pulse polarography in advanced oxidation processes for water treatment, *Journal of Water Process Engineering*, 53, 103707. https://doi.org/10.1016/j.jwpe.2023.103707

Dong, X-x., Li, M-y., Feng, N-n., Sun, Y-m., Yang, Ch. & Xu, Zh-l. (2015). A nanoporous MgO based nonenzymatic electrochemical sensor for rapid screening of hydrogen peroxide in milk, *RSC Advances*, 5(105), 86485.https://doi.org/10.1039/C5RA18560

Gizaw, Z. (2019), Public health risks related to food safety issues in the food market: a systematic literature review, *Environmental Health and Preventive Medicine*, 24(1), 68. https://doi.org/10.1186/s12199-019-0825-5

Guascito, M. R., Filippo, E., Malitesta, C., Manno, D., Serra, A. & Turco, A. (2008). A new amperometric nanostructured sensor for the analytical determination of hydrogen peroxide,

Biosensors and Bioelectronics, 24(4),1057–1063.

https://doi.org/10.1016/j.bios.2008.07.048

Harris, D. C. (2007). Quantitative chemical analysis ,7th Edition, W. H. Freeman.

Hu, A. L., Liu, Y. H., Deng, H. H., Hong, G. L., Liu, A. L., Lin, X. H., Xia, X. H. & Chen, W. (2014). Fluorescent hydrogen peroxide sensor based on cupric oxide nanoparticles and its application for glucose and L-lactate detection, *Biosensors and Bioelectronics*, 61, 374-378. https://doi.org/10.1016/j.bios.2014.05.048

Islas, M. S., Martínez Medina, J. J., Piro, O. E., Echeverría, G. A., Ferrer, E. G. & Williams, P. A. M. (2018). Comparisons of the spectroscopic and microbiological activities among coumarin-3-carboxylate, o-phenanthroline and zinc(II) complexes, *Spectrochimica Acta Part A: Molecular and Biomolecular Spectroscopy*, 198, 212-221.

https://doi.org/10.1016/j.saa.2018.03.003

Ivanova, A. S., Merkuleva, A. D., Andreev, S. V. & Sakharov, K. A. (2019). Method for determination of hydrogen peroxide in adulterated milk using high performance liquid chromatography, *Food Chemistry*. 283, 431-436. https://doi.org/10.1016/j.foodchem.2019.01.051

Kim, Y., Jeon, Y., Na, M., Hwang, S-J. & Yoon, Y. (2024). Recent trends in chemical sensors for detecting toxic materials, *Sensors*, 24(2), 431. https://doi.org/10.3390/s24020431

Li, P., Wang, Y., Liu, W., Chen, T. & Liu, K. (2025). Enhancing the structural and electrochemical properties of lithium iron phosphate via titanium doping during precursor synthesis, *Energies*, 2025, 18(4), 930. https://doi.org/10.3390/en18040930

Lima, L. S., Rossini, E. L., Pezza, L. & Pezza, H. R. (2020). Bioactive paper platform for detection of hydrogen peroxide in milk, *Spectrochimica Acta Part A*

Molecular and Biomolecular Spectroscopy, 227, 117774. https://doi.org/10.1016/j.saa.2019.117774

Liu, Sh. G., Liu, S., Yang, Sh., Zhao, Q., Deng, J. & Shi, X. (2022). A facile fluorescent sensing strategy for determination of hydrogen peroxide in foods using a nanohybrid of nanoceria and carbon dots based on the target-promoted electron transfer, *Sensors and Actuators B Chemical*, 356, 131325. https://doi.org/10.1016/j.snb.2021.131325

Masoud Shariati-Rad, M., Salarmand, N. & Jalilvand, F. (2017). Determination of hydrogen sulfide and hydrogen peroxide in complex samples of milk and urine by spectroscopic standard addition data and chemometrics methods, *RSC Advances*, 7, 28626-28636. https://doi.org/ 10.1039/C7RA00626H

Myers, J. N., Zhang, Ch., Chen, Ch. & Chen, Zh. (2014). Influence of casting solvent on phenyl ordering at the surface of spin cast polymer thin films, *Journal of Colloid and Interface Science*, 423, 60-66. https://doi.org/10.1016/j.jcis.2014.02.027

Mukhopadhya, A., Santoro, J. & Odriscoll, L. (2021). Extracellular vesicle separation from milk and infant milk formula using acid precipitation and ultracentrifugation. *STAR Protocols*, 2(4), 100821.

https://doi.org/10.1016/j.xpro.2021.100821

Nafradi, M., Farkas, L., Alapi, T., Hernadi, K., Kovacs, K., Wojnarovits, L. & Takacs E. (2020). Application of coumarin and coumarin-3-carboxylic acid for the determination of hydroxyl radicals during different advanced oxidation processes, *Radiation Physics and Chemistry*, 170, 108610.

 $https://doi.org/10.1016/j.radphyschem. 2019\\.108610$

Nitinaivinij, K., Parnklang, T., Thammacharoen, Ch., Ekgasit, S. & Wongravee, K. (2014). Colorimetric determination of hydrogen peroxide by morphological decomposition of silver nanoprisms coupled with chromaticity analysis, *Analytical Methods*, 6(24), 9816-9824.

https://doi.org/10.1039/C4AY02339K

Palsaniya, Sh., Jat, B. L. & Mukherji, S. (2023). Amperometry sensor for real time detection of hydrogen peroxide adulteration in food samples, *Electrochimica Acta*, 462, 142724.https://doi.org/10.1016/j.electacta.2 023.142724

Rutely-C, B. C., Jean-M, F., Walter-Z, T., Xochitled, D. B. & Mika, S. (2018). Towards reliable quantification of hydroxyl radicals in the Fenton reaction using chemical probes, *RSC Advances*, 8(10), 5321-5330.

https://doi.org/10.1039/c7ra13209c

Sadowska-Bartosz, I. & Bartosz G. (2025). Hydrogen peroxide: A ubiquitous component of beverages and food, *International Journal of Molecular Sciences*, 26(7):3397. https://doi.org/10.3390/ijms26073397

Thambiliyagodage, Ch., Jayanetti, M., Mendis, A., Ekanayake, G., Liyanaarachchi, H. & Vigneswaran, S. (2023). Recent advances in chitosan-based applications, A review, *Materials*, 16(5), 2073. https://doi.org/10.3390/ma16052073

Vasconcelos, H., Matias, A., Mendes, J., Araújo, J., Dias, B., Jorge, P. A.S., Saraiva, C., de Almeida, J. M. M. & Coelho, L. C.C. (2023). Compact biosensor system for the quantification of hydrogen peroxide in milk, *Talanta*, 253, 124062. https://doi.org/10.1016/j.talanta.2022.12406

Wang, X., Wolfbeis, O. S. & Meier, R. J. (2013). Luminescent probes and sensors for temperature. Chemical Society Reviews, 42(19), 7834-7869. https://doi.org/10.1039/c3cs60102a

Wang, Y., Xu, L. & Xie, W. (2019). Rapid and sensitive colorimetric sensor for

H₂O₂ and Hg²⁺ detection based on homogeneous iodide with high peroxidase-mimicking activity, *Microchemical Journal*, 147, 75-82. https://doi.org/10.1016/j.microc.2019.03.01

Zambrano, G., Nastri, F., Pavone, V., Lombardi, A. & Chino M. (2020). Use of an artificial miniaturized enzyme in hydrogen peroxide detection by chemiluminescence, *Sensors*, 20(13), 3793. https://doi.org/10.3390/s20133793

Zhang, X., Wang, S., Dao, J., Guo, J. & Gao Y. (2022) A colorimetric sensing platform for the determination of H₂O₂ using 2D–1D MoS₂-CNT nanozymes, *RSC*

Advances. 12(44), 28349-28358. https://doi.org/ 10.1039/d2ra04831k

Zhao, J., Wang, Y., Wang, T., Hasebe, Y. & Zhang, Zh. (2021). Molten-salt-composite of pyrite and silver nanoparticle as electrocatalyst for hydrogen peroxide sensing. *Analytical Sciences*. 37(11), 1589–1595.

https://doi.org/10.2116/analsci.21P119

Zhou, G., Wang, X. & Yang, Y. (2024). A new coumarin derivative as a highly selective 'turn-on' fluorescence probe for La³⁺ (lanthanum ion) in living zebrafish, *Journal of Photochemistry and Photobiology A Chemistry*, 447(7), 115264. https://doi.org/10.1016/j.jphotochem.2023. 115264